Molecular Cell
Article

Endothelin-1-Stimulated $InsP_3$-Induced Ca^{2+} Release Is a Nexus for Hypertrophic Signaling in Cardiac Myocytes

Daniel R. Higazi,[1,6] Claire J. Fearnley,[1,6] Faye M. Drawnel,[1] Amarnath Talasila,[1] Elaine M. Corps,[1] Oliver Ritter,[3] Fraser McDonald,[4] Katsuhiko Mikoshiba,[5] Martin D. Bootman,[1,*] and H. Llewelyn Roderick[1,2,*]
[1]Laboratory of Molecular Signalling, Babraham Institute, Cambridge CB22 3AT, UK
[2]Department of Pharmacology, University of Cambridge, Tennis Court Road, Cambridge CB2 1PD, UK
[3]Department of Medicine I, University of Wuerzburg, Josef Schneider Strasse 2, 97080 Wuerzburg, Germany
[4]Department of Orthodontics, Tower Wing, KCL, St. Thomas Street, London SE1 9RT, UK
[5]The Division of Molecular Neurobiology, The University of Tokyo, 4-6-1 Shirokanedai, Minato-ku, Tokyo 108-8639, Japan
[6]These authors contributed equally to this work
*Correspondence: martin.bootman@bbsrc.ac.uk (M.D.B.), llewelyn.roderick@bbsrc.ac.uk (H.L.R.)
DOI 10.1016/j.molcel.2009.02.005

SUMMARY

Ca^{2+} elevations are fundamental to cardiac physiology-stimulating contraction and regulating the gene transcription that underlies hypertrophy. How Ca^{2+} specifically controls gene transcription on the background of the rhythmic Ca^{2+} increases required for contraction is not fully understood. Here we identify a hypertrophy-signaling module in cardiac myocytes that explains how Ca^{2+} discretely regulates myocyte hypertrophy and contraction. We show that endothelin-1 (ET-1) stimulates $InsP_3$-induced Ca^{2+} release (IICR) from perinuclear $InsP_3$Rs, causing an elevation in nuclear Ca^{2+}. Significantly, we show that IICR, but not global Ca^{2+} elevations associated with myocyte contraction, couple to the calcineurin (CnA)/NFAT pathway to induce hypertrophy. Moreover, we found that activation of the CnA/NFAT pathway and hypertrophy by isoproterenol and BayK8644, which enhance global Ca^{2+} fluxes, was also dependent on IICR and nuclear Ca^{2+} elevations. The activation of IICR by these activity-enhancing mediators was explained by their ability to stimulate secretion of autocrine/paracrine ET-1.

INTRODUCTION

The heart is an extremely plastic organ that modifies its output to meet increased hemodynamic demands. Acutely, this is achieved by increasing the rate and force of contraction. Prolonged requirements for increased cardiac output are met by a compensated hypertrophic response, characterized by increased cell size rather than number, which serves to increase cardiac function (Lorell and Carabello, 2000; Dorn and Force, 2005). Although this compensated response provides for the greater requirements of athletes or expectant mothers, under certain pathological conditions, cardiac hypertrophy can become decompensated, manifesting itself in decreased cardiac output that can lead to death (Lorell and Carabello, 2000; Allender et al., 2006).

Ca^{2+} has a fundamental role in the biology of cardiac myocytes—stimulating their contraction during every heartbeat as well as the transcription of genes involved in cardiac hypertrophy (Frey et al., 2000; Bers, 2002; Molkentin, 2006). Many of the pro-hypertrophic effects of Ca^{2+} are mediated through the EF-hand-containing Ca^{2+} sensor protein calmodulin (CaM) (Obata et al., 2005; Heineke and Molkentin, 2006). Ca^{2+}/CaM, in turn, either directly interacts with transcriptional modulators such as the CaM-binding transcription activator (CAMTA) (Song et al., 2006), or as for type 2 histone deacetylases (HDACs) and NFAT (Molkentin et al., 1998; Zhang et al., 2002a), regulates their activity via Ca^{2+}-sensitive enzymes that include Ca^{2+}/CaM kinase II (CaMKII) and calcineurin (CnA), respectively (Frey et al., 2000; Heineke and Molkentin, 2006). Despite identifying these Ca^{2+} targets and their mechanisms of action, it remains to be fully established how Ca^{2+} can act with such great specificity and fidelity to control transcription on the background noise of the global Ca^{2+} signals associated with every heartbeat.

To achieve this specificity, it has been suggested that stress/workload-induced changes in the frequency, shape, or amplitude of excitation contraction coupling (ECC)-associated Ca^{2+} transients could encode information that would induce hypertrophic gene transcription (Berridge et al., 2003). Alternatively, altered Ca^{2+} signals could act coincidently with other signaling mediators, such as MAPK and PKB, which are also activated under hypertrophic conditions (Heineke and Molkentin, 2006). A further possibility that has gained recent support is that Ca^{2+} signals generated via mechanisms distinct from ECC control hypertrophic gene transcription. For example, by Ca^{2+} entry through TRPC cation channels on the plasma membrane (Kuwahara et al., 2006; Nakayama et al., 2006; Brenner and Dolmetsch, 2007) or by Ca^{2+} signals arising from endoplasmic reticulum (ER)/sarcoplasmic reticulum (SR) $InsP_3$ receptor ($InsP_3R$) Ca^{2+} channels (Perez et al., 1997; Lipp et al., 2000; Wu et al., 2006; Zima et al., 2007). The stimulation of $InsP_3$-induced Ca^{2+} release (IICR) downstream of plasma membrane receptors, such as the

$G\alpha_q$-linked endothelin receptor (ET_AR) that also promote hypertrophy, further supports the idea that IICR is a regulator of hypertrophic gene transcription (Mackenzie et al., 2002; Zima and Blatter, 2004). Indeed, a recent study showed that IICR could activate CaMK, causing export of an exogenously expressed GFP-HDAC and induction of a synthetic myocyte enhancer factor 2 (MEF2) reporter in cardiac myocytes (Wu et al., 2006). These data were extrapolated to suggest that IICR was a regulator of myocyte hypertrophy. As no bona fide markers of hypertrophy were assessed, further analysis of the role of IICR in this process is required.

Here, we set out to test the hypothesis that IICR provides a discrete signaling mechanism to control hypertrophic gene transcription independently of the Ca^{2+} transients associated with ECC. Since IICR has now been widely reported in cardiac myocytes (Kockskamper et al., 2008), regulating both ECC and stimulating arrhythmogenic Ca^{2+} signals, we also set out to establish whether IICR represented a conserved signaling mechanism employed in the induction of hypertrophy. Specifically, whether it is employed by diverse hypertrophic stimuli and not solely by hypertrophic agents that engage phospholipase C (PLC)-coupled plasma membrane receptors. To these ends, we examined the distinct roles of $InsP_3$-stimulated Ca^{2+} elevations versus those arising due to ECC in the induction of hypertrophy. We also investigated under what conditions IICR is employed to induce hypertrophy, and the mechanism(s) by which IICR can engage the transcriptional machinery. Our results show that $InsP_3$-stimulated increase in nuclear Ca^{2+} and its engagement of the CnA/NFAT pathway is a requisite and conserved signal for the induction of hypertrophy by both neurohumoral and activity-inducing stimuli in cardiac myocytes. Moreover, we show that activity-induced secretion of paracrine/autocrine endothelin-1 (ET-1) serves to create a link between myocyte activity/workload and the induction of cardiac hypertrophy.

RESULTS

ET-1 Promotes Hypertrophy in an IICR-Dependent Manner

Application of ET-1 for 24 hr to cultures of spontaneously beating neonatal rat ventricular myocytes (NRVMs) induced a characteristic hypertrophic effect (Figure 1A) as determined using a number of well-characterized hallmarks. A principal marker of hypertrophy used in this study, which has been extensively validated in a number of different hypertrophy models, was atrial natriuretic factor (ANF) (Shubeita et al., 1990; Aronow et al., 2001). Cell surface area measurements were also used as an obvious physical characteristic of hypertrophy. ANF expression was quantitated by counting ANF immunoreactive myocytes and by quantitative real-time PCR (Figure 1A). α-actinin staining also showed increased organization following ET-1 stimulation.

ET-1 promotes both IICR and modulates Ca^{2+} transients associated with ECC (Figure 1B) (Wu et al., 2006; Kockskamper et al., 2008). Here we investigated the discrete contributions of IICR and the Ca^{2+} transients associated with ECC to the prohypertrophic action of ET-1 (Figure 1B). Ca^{2+} imaging of NRVMs revealed spontaneous Ca^{2+} transients that were significantly increased in frequency following ET-1 application (Figure 1C). This chronotropic action of ET-1 was not dependent upon $InsP_3$ signaling, since it was unaffected by expression of the type 1 $InsP_3$ 5′-phosphatase, which metabolizes $InsP_3$ to $InsP_2$ (Figure 1C), or application of the $InsP_3R$ antagonist 2-APB (Mackenzie et al., 2002) (data not shown). In cells in which ECC was blocked with nifedipine and mibefradil, antagonists of L-type and T-type channels, respectively (“ECC blocked”) (Escobar et al., 2004), ET-1 induced an elevation of intracellular Ca^{2+} that was sensitive to expression of $InsP_3$ 5′-phosphatase or 2-APB (Figure 1D and data not shown). In summary, these data show that ET-1 promotes IICR and increases the frequency of ECC-associated Ca^{2+} transients, although the latter effect is independent of IICR.

We next investigated whether inhibition of IICR affected ET-1-stimulated hypertrophy. Intriguingly, inhibition of IICR with $InsP_3$ 5′-phosphatase or 2-APB abrogated the hypertrophic response (Figures 1E and Figure S1 [available online]).

To assess whether hypertrophic remodeling was induced by coincident ET-1-stimulated IICR and enhanced ECC, and to determine whether IICR was necessary for hypertrophic remodeling, the effect of ET-1 was measured in myocytes in which ECC was blocked. Under these conditions, despite the absence of ECC-associated global Ca^{2+} transients, ET-1 retained its ability to induce hypertrophy. Moreover, hypertrophy was again sensitive to $InsP_3$ 5′-phosphatase expression (Figure 1F). 2-APB application also significantly reduced the ET-1-stimulated increase in the percentage of ANF-positive NRVMs under ECC-blocked conditions from 56.80% ± 3.77% to 43.79% ± 2.84% ($p < 0.007$). Together, these data indicate that ET-1 stimulated hypertrophy is dependent upon IICR but not ECC.

ET-1 and $InsP_3$ Ester Stimulate Increases in Nuclear Ca^{2+}

The sensitivity of ET-1-stimulated hypertrophy, but not chronotropy, to inhibition of $InsP_3$ signaling may appear discordant. To rationalize these findings, we hypothesized that ET-1 was promoting IICR in a microdomain that was spatially distinct from the Ca^{2+} changes that were occurring during ECC, and that this Ca^{2+} signal was insufficient to modify ECC but sufficient to drive hypertrophic gene transcription. The confocal imaging data in Figure 2A indicated that, during ECC, Ca^{2+} levels increased throughout the cell, whereas under conditions where ECC was blocked, ET-1 and cell-permeant $InsP_3$ ester both promoted Ca^{2+} increases that were constrained to the nucleus (Figure 2A). The $InsP_3$-dependent Ca^{2+} increases correlated with the subcellular localization of type 2 $InsP_3$Rs ($InsP_3$R2), which were enriched in the perinuclear region of the cardiac myocytes, thus providing a mechanism for the generation of localized $InsP_3$-signaling events (Figure 2B). The restricted distribution of $InsP_3$Rs contrasts with that of type 2 RyRs (RyR2), which were expressed throughout the cell, raising the possibility that $InsP_3$Rs have a specialized function in cardiac myocytes (Figure 2B).

The requirement for nuclear Ca^{2+} signals for ET-1-stimulated ANF expression was next probed. To this end, nuclear Ca^{2+} was specifically buffered using a nuclear-targeted, red fluorescent protein (mRFP)-tagged form of the neuronal Ca^{2+} binding protein calbindin (CB-NLS). Significantly, CB-NLS expression abrogated ET-1-induced ANF expression in ECC-blocked myocytes, as well as in myocytes that were spontaneously active

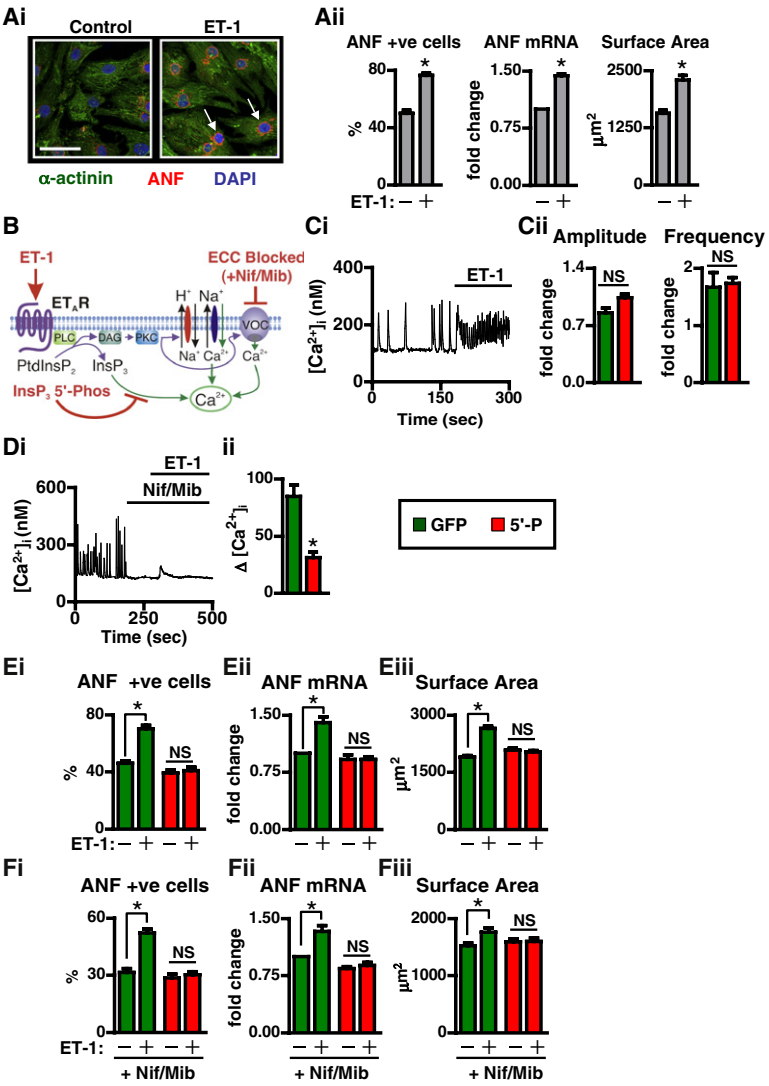

Figure 1. IICR Is Required for ET-1-Stimulated Hypertrophic Remodeling

(A) (Ai) Confocal images of neonatal myocytes treated ± ET-1 (100 nM; 24 hr) and then immunostained with antibodies to ANF (red) and α-actinin (green). Nuclei are indicated by the blue DAPI staining. White arrows indicate perinuclear rings of ANF. Scale bar represents 50 μm. (Aii) Quantitation of ANF-expressing NRVMs, ANF mRNA abundance, and cell surface area following 24 hr exposure to ET-1.

(B) Schematic of the Ca^{2+} pathways activated by ET-1 in cardiac myocytes and interventions imposed to inhibit ECC (+Nif/Mib indicates nifedipine and mibefradil application) and IICR ($InsP_3$ 5′-Phos). VOC is an abbreviation of voltage-operated channel.

(C) Effect of $InsP_3$-5′-phosphatase expression upon ET-1-stimulated changes in Ca^{2+} signals in NRVMs. (Ci) Ca^{2+} recording from a spontaneously beating NRVM stimulated with ET-1 (100 nM). (Cii) Fold changes in amplitude and frequency of the Ca^{2+} transients in GFP- and $InsP_3$ 5′-phosphatase-expressing NRVMs following ET-1 stimulation.

(D) Effect of $InsP_3$ 5′-phosphatase expression upon ET-1-stimulated Ca^{2+} changes in NRVMs in which ECC was blocked. (Di) Ca^{2+} recording in NRVM under the conditions indicated. (Dii) Assessment of the effect of $InsP_3$ 5-phosphatase expression upon ET-1-stimulated Ca^{2+} increases shown in (Di).

(E) Quantitation of hypertrophic remodeling in spontaneously active NRVMs exposed to the conditions shown. Histograms describe the percentage of ANF-positive myocytes (Ei), ANF mRNA abundance (Eii), and cell surface area (Eiii).

(F) Quantitation of the effect of $InsP_3$ 5′-phosphatase expression upon ET-1-stimulated hypertrophic remodeling in NRVMs in which ECC was blocked. The percentage of ANF-expressing myocytes (Fi), ANF mRNA abundance (Fii), and cell surface area (Fiii) are shown. Experiments were performed on a minimum of three occasions. Data are presented as mean ± SEM. Asterisk indicates statistical significance at $p < 0.05$. NS, not significant.

(Figures 2C and 2D). As the expression of CB-NLS only inhibited increases in nuclear Ca^{2+}, even in spontaneously beating myocytes experiencing large cytosolic Ca^{2+} fluxes (Figure S2), these data indicated that elevations in nuclear Ca^{2+} were required for the induction of ANF expression by ET-1.

Since the CnA/NFAT pathway has been shown to mediate the gene transcription required for pathological hypertrophy (Wilkins et al., 2004), we next tested whether it was activated by IICR and was involved in IICR-induced ANF expression. To this end, CnA was inhibited with cyclosporin A (CsA), and NFAT activation by CnA was prevented using a cell-permeant VIVIT peptide (Aramburu et al., 1999). Both treatments significantly reduced ET-1-stimulated ANF expression in cells in which ECC was blocked (Figure 3A). The activity of an NFAT-luciferase reporter was also induced by ET-1 stimulation in ECC-blocked cells (2.2 ± 0.46-fold increase from control; $p < 0.05$, $n = 4$). Having shown that ET-1-stimulated ANF expression was CnA/NFAT-dependent under conditions where ECC was absent (only ET-1-stimulated IICR), we next tested whether IICR was sufficient for nuclear translocation of NFAT. ET-1 stimulated the nuclear accumulation of GFP-tagged NFAT-C1 in an $InsP_3$ 5′-phosphatase-sensitive manner (Figure 3B). Moreover, even in myocytes experiencing ECC-associated global Ca^{2+} signals, ET-1-stimulated NFAT-C1 nuclear translocation was sensitive to $InsP_3$ 5′-phosphatase expression (Figure 3B).

The important role of ET-1-stimulated IICR in the nucleus for the activation of the CnA/NFAT pathway was further substantiated by the decrease in ET-1-induced ANF expression observed in myocytes treated with a cell-permeant peptide inhibitor of CnA nuclear translocation (Hallhuber et al., 2006) (Figure 3C). Together, these data show that ET-1 induces hypertrophy by causing $InsP_3$-stimulated increases in nuclear Ca^{2+}, which activates the CnA/NFAT pathway.

IICR Is an Obligate Signal for Workload-Induced Hypertrophy

The role of $InsP_3$ signaling in hypertrophy induced by the β-adrenergic agonist isoproterenol or the L-type channel agonist

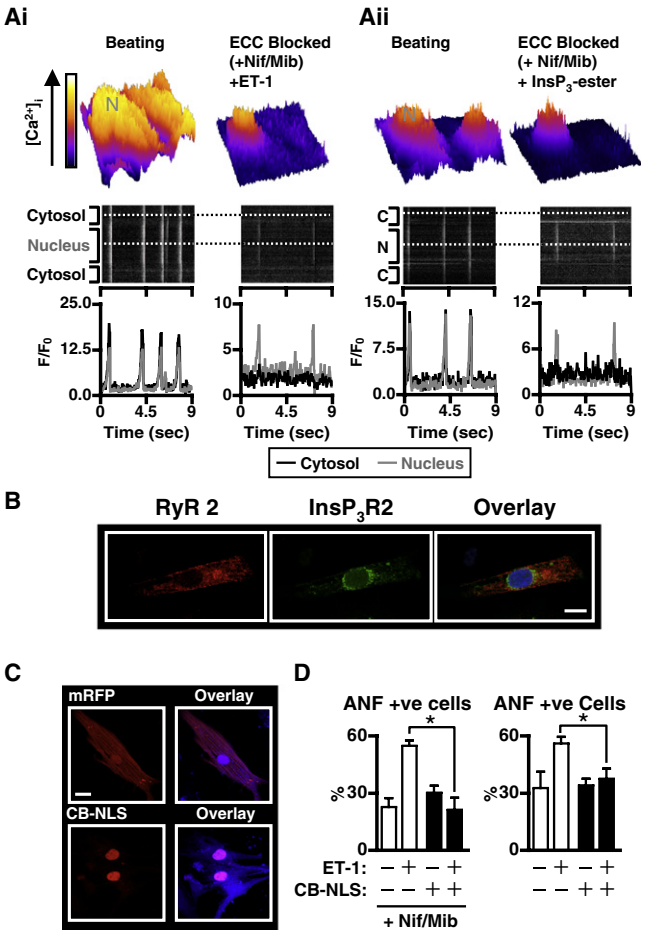

Figure 2. ET-1-Stimulated $InsP_3$-Dependent Elevations in Nuclear Ca^{2+} that Are Required for Its Induction of ANF Expression

(A) ET-1 and $InsP_3$-ester induce nuclear-specific Ca^{2+} signals in NRVMs. (Ai and Aii) The upper panels show surface plots of fluo-4 intensity in either spontaneously beating or ECC-blocked myocytes treated ± ET-1 or $InsP_3$-ester. Images of two myocytes are shown in each case. N indicates the position of the nucleus. The middle panels show the corresponding time projections of intensity from a 10 pixel wide line drawn across the cell through the center of the nucleus. The positions of the nucleus (N) and cytosol (C) are shown. The lower panel shows plots of fluo-4 fluorescence taken from the dashed lines shown in the middle panel.

(B) Confocal images of NRVMs labeled with antibodies directed against the type 2 RyR (red) and the $InsP_3R2$ (green). Scale bar represents 10 μm.

(C) Confocal images of NRVMs transfected with mRFP or mRFP-CB-NLS (CB-NLS; both in red). Myocytes are counterstained with an antibody against α-actinin and with DAPI (cytosol and nuclei stained; both in blue). Scale bar represents 20 μm.

(D) Quantitation of ET-1-stimulated ANF expression in myocytes expressing either mRFP or CB-NLS. Data are presented as mean ± SEM. Asterisk indicates statistical significance at $p < 0.05$.

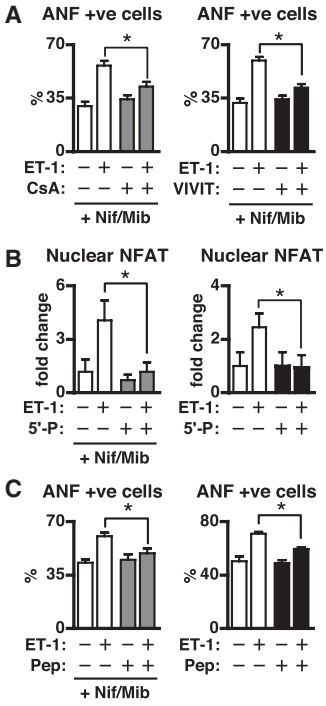

Figure 3. ET-1-Stimulated IICR Engages the CnA/NFAT Pathway

(A) Quantitation of ANF expression in ECC-blocked NRVMs stimulated with ET-1 and treated with either CsA (500 nM, 30 min pretreatment; left panel) or cell-permeant VIVIT (2 μM, 30 min pretreatment; right panel).

(B) Effect of $InsP_3$ 5′-phosphatase on ET-1-stimulated increases in NFAT nuclear accumulation in ECC-blocked and spontaneously active myocytes. Fold changes in the percentage of myocytes expressing GFP-NFATC1 in the nucleus are shown.

(C) Quantitation of ANF immunoreactive myocytes following ET-1 stimulation and application of a cell-permeant peptide (pep; 1 μM, 4 hr pretreatment) inhibitor of CnA nuclear import. Data are presented as mean ± SEM. Asterisk indicates statistical significance at $p < 0.05$.

BayK8644 was next investigated. Both of these agents act to increase Ca^{2+} cycling, thereby mimicking increased workload (Figures 4A and 4B). BayK8644 was used, as it acts solely to enhance Ca^{2+} fluxes through the L-type channel and could therefore control for Ca^{2+}-independent actions of β adrenergic stimulation. The potent modification of Ca^{2+} cycling by these agents was insensitive to $InsP_3$ 5′-phosphatase expression, indicating that their enhancement of ECC was independent of the $G\alpha_q$-$InsP_3$-signaling pathway (Figure 4C). However, BayK8644- and isoproterenol-stimulated increases in ANF expression and cell size were inhibited by expression of $InsP_3$ 5′-phosphatase (Figure 4D). Moreover, BayK8644-stimulated NFAT nuclear accumulation was also significantly reduced by $InsP_3$ 5′-phosphatase expression (10.18 ± 0.53-fold increase over controls in BayK8644-treated cells versus 6.723 ± 1.03 in $InsP_3$ 5′-phosphatase-expressing BayK8644-treated cells, $n = 9$; $p < 0.05$). As the BayK8644- and isoproterenol-mediated enhancement of ECC was not affected by $InsP_3$ 5′-phosphatase expression (Figures 4Ci and 4Cii), these data indicated that ANF expression and NFAT nuclear translocation were not directly regulated by ECC-associated Ca^{2+} oscillations.

Autocrine/Paracrine Signaling Involving ET-1 Drives IICR and Hypertrophy

Since ET-1 is known to signal in a paracrine/autocrine manner in cardiac myocytes (Ergul et al., 2000; Motte et al., 2003), we next investigated whether this contributed to the $InsP_3$ dependence

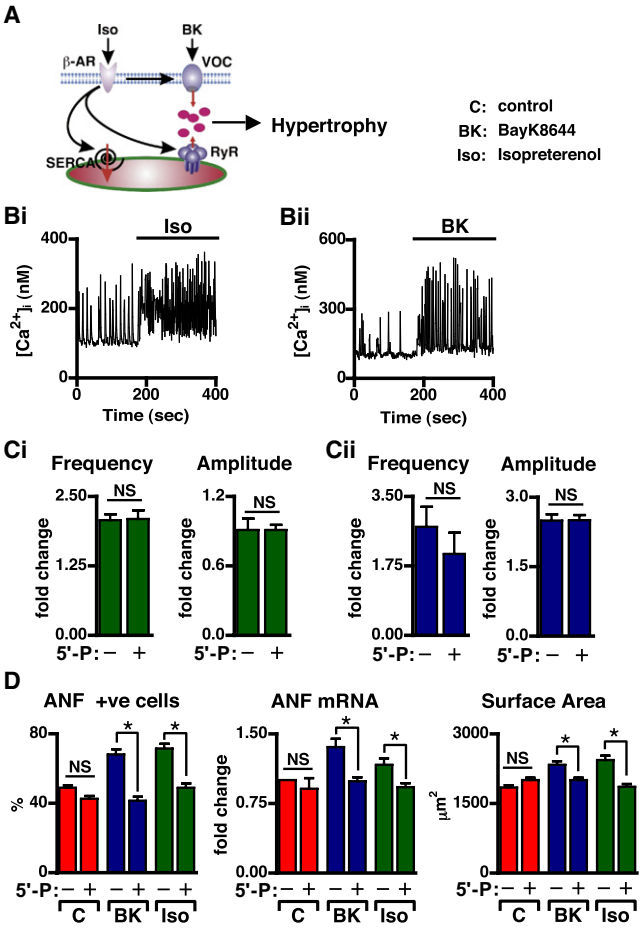

Figure 4. Enhanced ECC Induces Hypertrophic Remodeling in an $InsP_3$-Dependent Manner

(A) Experimental manipulations used to increase myocyte activity/ECC.

(B) Ca^{2+} recordings in spontaneously beating NRVMs stimulated with isoproterenol (Iso; [Bi]) or BayK8644 (BK; [Bii]).

(C) Effect of $InsP_3$ 5′-phosphatase expression upon isoproterenol (Ci)- or BayK8644 (Cii)-induced changes in amplitude and frequency of Ca^{2+} signals in spontaneously beating NRVMs.

(D) Quantitation of hypertrophic remodeling in NRVMs exposed to the conditions shown. Histograms show the percentage of ANF-positive myocytes, ANF mRNA abundance, and cell surface area. 5′-P indicates expression of $InsP_3$ 5′-phosphatase. GFP was expressed in controls. Data are presented as mean ± SEM. Asterisk indicates statistical significance at $p < 0.05$.

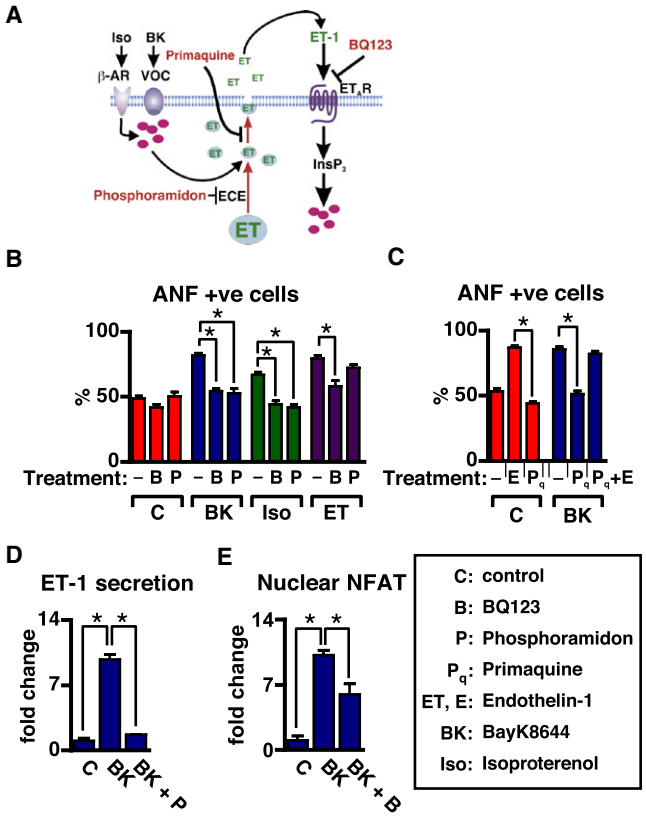

Figure 5. An Autocrine/Paracrine Pathway Involving Secretion of ET-1 Underlies Induction of ANF Expression by Enhanced ECC

(A) Schematic of the pathways that link Ca^{2+} signals and ET-1. The agents used to intervene in ET-1 processing and signaling and their sites of action are also shown.

(B) Histogram showing the effect of BQ123 (B) and phosphoramidon (P) upon the percentage of ANF-expressing myocytes induced by BayK8644 (BK), isoproterenol (Iso), or ET-1 (ET).

(C) Histogram showing the effect of primaquine (P_q) upon BayK8644-stimulated increase in the percentage of ANF-expressing cells. The effects of ET-1 (E) upon control and primaquine-treated BayK8644-stimulated myocytes are also shown.

(D) Quantitation of ET-1 levels in the media overlying cultures of NRVMs. The fold change between control and test conditions is presented.

(E) Histogram showing the effect of BayK8644 ± BQ123 upon the percentage of myocytes with nuclear NFAT. Data are presented as mean ± SEM. Asterisk indicates statistical significance at $p < 0.05$.

of BayK8644- and isoproterenol-induced hypertrophy (Figure 5A). Application of the selective ET_AR antagonist BQ123 (Russell and Molenaar, 2000) completely abolished the prohypertrophic effects of both isoproterenol and BayK8644 (Figure 5B). The ET-1-stimulated enhancement of ECC-associated Ca^{2+} transients and IICR were both inhibited by BQ123, indicating that the effects of ET-1 on Ca^{2+} were mediated by ET_AR and that BQ123 was an effective antagonist of ET-1 in these cells (Figure S2). BayK8644-induced enhancement of ECC was unaffected by BQ123, indicating that the effect of BQ123 was specific to the ET-1 signaling cassette (Figure S2).

To further test the paracrine/autocrine action of ET-1, inhibitors of its processing and secretion were employed (Figure 5A). Phosphoramidon, which inhibits ET-1 processing by endothelin-converting enzyme, significantly suppressed the prohypertrophic actions of BayK8644 and isoproterenol (Figure 5B). The specificity and lack of toxicity of phosphoramidon were validated by the induction of ANF expression in phosphoramidon-treated cells by exogenous ET-1 (Figure 5B). Inhibition of secretion with primaquine (Hiebsch et al., 1991) also abrogated BayK8644-induced hypertrophy (Figure 5C). This inhibitory effect of primaquine upon BayK8644-induced ANF expression was rescued by application of exogenous ET-1, indicating that it was affecting ET-1 secretion, not ET-1 signaling (Figure 5C). Moreover, primaquine did not affect spontaneous Ca^{2+} transients (data not shown). Further evidence in favor of an autocrine/paracrine

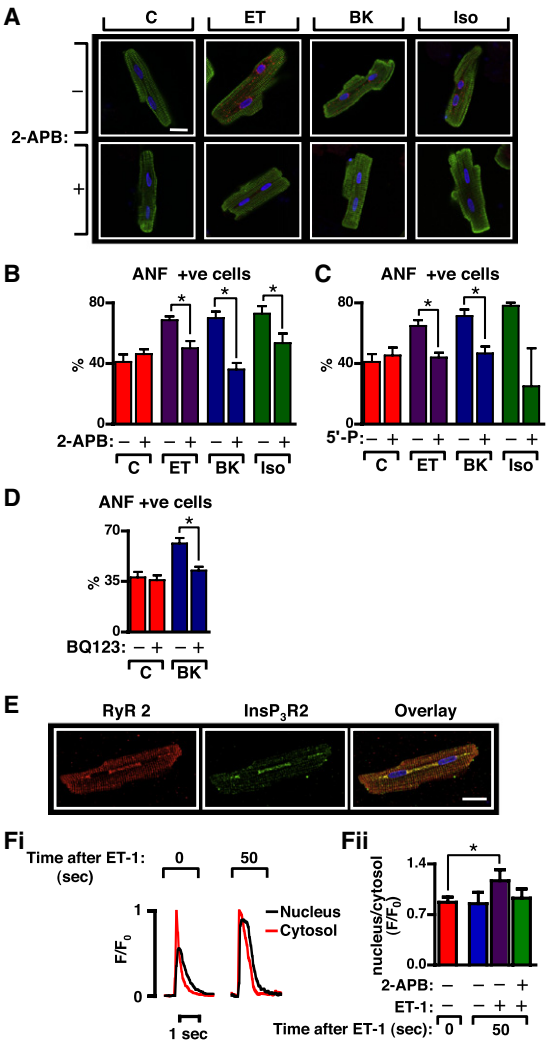

Figure 6. Autocrine/Paracrine ET-1 and $InsP_3$ Signaling Are Required for Induction of ANF Expression in ARVMs

(A) Confocal images of ARVMs captured following 24 hr culture in the agents indicated. ANF is shown in red, α-actinin is shown in green, and nuclei are indicated by the blue DAPI staining. Scale bar represents 20 μm.

(B and C) Quantitation of the effects of 2-APB (B) or $InsP_3$ 5′-phosphatase expression (C) upon the percentage of myocytes expressing ANF following 24 hr exposure to ET-1, BayK8644, or isoproterenol. Controls in the 5′-phosphatase experiments express GFP.

(D) Effect of BQ123 upon BayK8644-induced increases in the percentage of ANF-expressing myocytes.

(E) Confocal image of an ARVM immunostained with antibodies against RyR2 (red) and $InsP_3R2$ (green). Nuclei are indicated by the blue DAPI staining. Scale bar represents 10 μm.

(F) Confocal imaging of Ca^{2+} in the cytosol and nucleus of paced ARVMs. (Fi) Normalized traces illustrating nuclear and cytosolic Ca^{2+} prior to ET-1 application and 50 s after ET-1 application. (Fii) Summarized nuclear:cytosolic ratio of F/F_0 normalized to prestimulation conditions. Data are presented as mean ± SEM. Asterisk indicates statistical significance at $p < 0.05$.

action of ET-1 was provided by the significant increase in ET-1 detected in medium overlying the neonatal myocytes following application of BayK8644 for 24 hr (Figure 5D). The BayK8644-stimulated increase in ET-1 was prevented by coapplication of phosphoramidon (Figure 5D). BQ123 application also significantly reduced the nuclear accumulation of NFAT in BayK8644-stimulated cells (Figure 5E). Together, these data are consistent with a model in which myocyte activity promotes ET-1 secretion, which then acts in an autocrine/paracrine manner and signals via IICR and CnA/NFAT to induce ANF expression.

ET-1-Stimulated IICR Underlies Hypertrophic Remodeling in Myocytes Isolated from Adult Rats

The role of IICR and autocrine/paracrine ET-1 signaling in hypertrophic signaling was also examined in adult rat ventricular myocytes (ARVMs). As observed in NRVMs, ET-1, BayK8644, and isoproterenol also potently induced ANF expression in ARVMs (Figures 6A–6C). Moreover, the effect of these agents on the induction of ANF expression was significantly reduced by abrogation of IICR by $InsP_3$ 5′-phosphatase expression or 2-APB treatment. Consistent with the data in NRVMs, BayK8644-induced ANF expression in ARVMs was also BQ123 sensitive (Figure 6D). Mirroring the data in NRVMs, type 2 $InsP_3Rs$ were in greatest abundance in a region that surrounded and spanned between the two nuclei (Figure 6E). As we have previously shown (Mackenzie et al., 2002), some $InsP_3Rs$ were also present near the sarcolemma and on the striations that indicate the sarcoplasmic reticulum. The RyRs, in contrast, were distributed in a striated pattern throughout the cytoplasm.

Confocal Ca^{2+} imaging of paced ARVMs revealed an ET-1-stimulated increase in nuclear Ca^{2+}, relative to cytosolic Ca^{2+} (Figure 6F). The ET-1-induced increase in nuclear to cytosolic Ca^{2+} ratio was 2-APB sensitive and therefore likely due to ET-1-mediated activation of nuclear $InsP_3Rs$.

DISCUSSION

The data presented in this study provide insights into the mechanisms that allow discrimination between Ca^{2+} signals that induce contraction and those that stimulate hypertrophy in cardiac myocytes. Specifically, they shed light on the fundamental role of and differences between neurohormonally stimulated IICR and ECC-associated Ca^{2+} signals, and their respective Ca^{2+} sources, in regulating cardiac hypertrophy. Together, our data show that IICR and its activation of the CnA/NFAT pathway is a signaling nexus in the transduction mechanism of different hypertrophic stimuli (Figure 7).

Many lines of evidence have implicated Ca^{2+} in the regulation of cardiac hypertrophy (Heineke and Molkentin, 2006). Indeed, as Ca^{2+} signaling is acutely modified to regulate cardiac output, a possible role for Ca^{2+} in regulating hypertrophic growth is easy to understand: more work, more activity, more heart (Bers, 2002). Despite significant research, the precise mechanism by which hypertrophy is regulated by Ca^{2+} remains widely debated (Molkentin, 2006).

Here we establish a model that places IICR as a common and requisite signaling module for the induction of hypertrophy by stimuli that directly activate $InsP_3$ production, as well as those that increase myocyte activity through the enhancement of ECC (Figure 7). Using a number of approaches to manipulate $InsP_3$ signaling in intact cells, we determined that hypertrophy is induced in an IICR-dependent manner by ET-1, the β-agonist

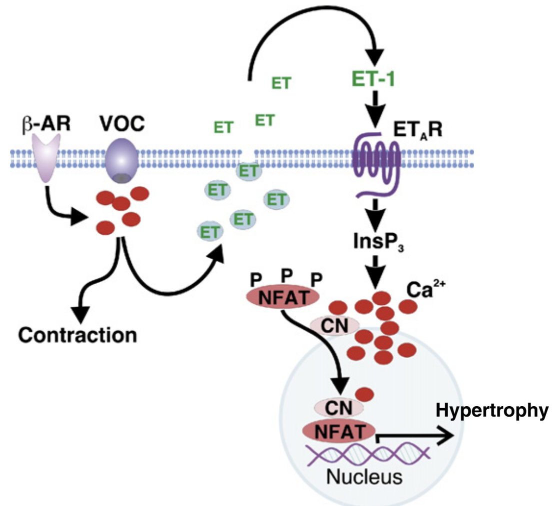

Figure 7. Model Depicting the Mechanism by which ET-1-Stimulated IICR Coordinates Hypertrophic Signaling

Engagement of ET receptors stimulates an increase in intracellular $InsP_3$, which mobilizes Ca^{2+} from a perinuclear SR/ER Ca^{2+} store, causing Ca^{2+} to increase in the nucleus. IICR engages the CnA/NFAT signaling pathway to induce hypertrophic remodeling. The effect of IICR is in part mediated by $InsP_3$-stimulated increases in nuclear Ca^{2+} sustaining NFAT nuclear localization by maintaining an interaction between CnA and NFAT. This ET-1/$InsP_3$/Ca^{2+}/CnA/NFAT pathway is also engaged following increases in myocyte work rate brought about through β-adrenergic receptor engagement or enhanced Ca^{2+} entry through L-type voltage-operated channels. This enhanced Ca^{2+} cycling promotes ET-1 secretion, which then acts on its cognate receptor to activate the prohypertrophic pathway described above.

isoproterenol, and the L-type channel agonist BayK8644. Although these agonists all elicited a chronotropic effect, this did not contribute to their prohypertrophic action. Moreover, ET-1-induced IICR promoted hypertrophy in the absence of ECC-associated Ca^{2+} transients. Although ET-1, acting via its $G\alpha_q$-coupled receptor, is capable of promoting IICR in cardiac myocytes (Mackenzie et al., 2002; Zima and Blatter, 2004), it was not clear how isoproterenol and BayK8644 could engage IICR. These agents were shown to elicit IICR by promoting ET-1 secretion, which then acted in an autocrine/paracrine manner to induce hypertrophy (Figure 7). Interestingly, in a recent study, HDAC5 nuclear export (which was used as a surrogate for hypertrophy) was shown to be induced by IICR but not ECC-mediated Ca^{2+} fluxes generated by electrical pacing (Wu et al., 2006). From these data, it was concluded that increased activity could not induce hypertrophy. However, as described above, measuring ANF expression and myocyte size in both neonatal and adult myocytes as more bona fide indices of hypertrophy, we revealed that hypertrophy *was* sensitive to increased activity. Due to the extended time course of our experiments (compared to the Wu et al. study), myocytes had sufficient time to elicit an autocrine/paracrine response involving ET-1, thereby allowing increased Ca^{2+} cycling to drive hypertrophy by recruiting IICR. Our conclusions that ET-1-stimulated IICR is a conserved signaling module employed in regulating hypertrophy is also supported by the lack of hypertrophy in mice in which components of the ET system have been genetically ablated (Wettschureck et al., 2001; Shohet et al., 2004). It is also interesting to note that ET-1 secretion and biosynthesis, as well as ET_AR levels, are upregulated in a number of cardiac disease models (Zolk et al., 2002; Motte et al., 2003).

The specific prohypertropic action of IICR prompted us to investigate the mechanism that allows prohypertrophic signal transducers to discriminate between IICR and enhanced ECC-associated Ca^{2+} transients downstream of ET-1 stimulation. We showed that $InsP_3Rs$ are localized around the nucleus, and in response to cellular stimulation with a physiological agonist or $InsP_3$ they release Ca^{2+} into a microdomain surrounding or within the nucleus, causing an increase in nuclear Ca^{2+}. These findings are consistent with a small but growing body of evidence demonstrating that IICR can occur in the nuclear region of primary cardiac myocytes (Wu et al., 2006; Heidrich et al., 2008; Kockskamper et al., 2008). Significantly, we were also able to demonstrate in cells expressing a nuclear-localized Ca^{2+} buffer that this elevation in nuclear Ca^{2+} elicited by $InsP_3$ was required for the induction of hypertrophy by ET-1. Moreover, buffering nuclear Ca^{2+} prevented ET-1-stimulated ANF expression not only in myocytes in which IICR was the only Ca^{2+} signal but also in spontaneously active myocytes experiencing global ECC-associated Ca^{2+} fluxes. Together, these observations lead us to suggest that Ca^{2+} signals emanating from $InsP_3Rs$ occur in a privileged nuclear microdomain appropriate to drive transcription, whereas Ca^{2+} signals that arise as a result of ECC do not. These findings are analogous to that observed in neurons and skeletal muscle cells where nuclear Ca^{2+} changes have been proposed to specifically regulate gene transcription (Hardingham et al., 1997; Cardenas et al., 2005).

In this manuscript, we identify the CnA/NFAT pathway as a key mechanism by which the requisite $InsP_3$-stimulated increase in nuclear Ca^{2+} couples to the transcriptional machinery to induce hypertrophy. As the CnA/NFAT pathway is an established mediator of pathological hypertrophy, these findings are particularly important and uncover a signaling link to NFAT activation (Molkentin et al., 1998; Wilkins et al., 2004). More significantly, as a result of buffering nuclear Ca^{2+} or inhibiting IICR, we were able to show that the enhanced ECC-associated global Ca^{2+} transients generated following stimulation with hypertrophic agonists, including ET-1, isoproterenol, and BayK8644, do not provide the Ca^{2+} signals that cause activation of the CnA/NFAT pathway. Rather, these stimuli, either directly, as for ET-1, or indirectly via secretion of autocrine/paracrine ET-1, as for isoproterenol and BayK8644, promote IICR, which then through an elevation in nuclear Ca^{2+} activates the CnA/NFAT pathway. It is important to note that our conclusions for this role of the CnA/NFAT pathway are based on analysis of the role of the CnA/NFAT pathway on the ET-1-stimulated induction of expression of a bona fide hypertrophy-associated protein (ANF) (Aronow et al., 2001), as well on the effect of IICR and nuclear Ca^{2+} transients on the activation of an NFAT-luciferase reporter and NFAT translocation. Together, these findings showing that the NFAT pathway is activated in an IICR-dependent manner by different hypertrophic stimuli provide insight into the mechanisms by which these diverse stimuli can utilize Ca^{2+} to induce hypertrophy. The employment of IICR to induce the CnA/NFAT pathway to promote hypertrophic gene transcription is an attractive model, as due to its kinetics of activation and deactivation,

control by ECC-mediated Ca^{2+} changes alone would render NFAT constitutively nuclear and active (Tomida et al., 2003). The requirement for additional Ca^{2+} signals provided by IICR would endow greater specificity and room for modulation. Although previous reports have suggested that NFAT is a simple integrator of the frequency of Ca^{2+} oscillations (Colella et al., 2008), our data would suggest a more complex scenario requiring autocrine/paracrine ET-1 signaling and IICR to maximally activate NFAT-mediated transcription. Indeed, although inhibition of IICR or ET_AR completely inhibited BayK8644- or ET-1-stimulated ANF expression, these maneuvers did not fully prevent BayK8644-stimulated nuclear accumulation of NFAT.

Our data showing the importance of nuclear Ca^{2+} in the regulation of the CnA/NFAT pathway are consistent with the reports in T lymphocytes that sustained elevation in Ca^{2+} is required for optimal induction of gene transcription by NFAT (Feske et al., 2000). Although sustained NFAT activity could be mediated by prolonged elevations in cytosolic Ca^{2+} and CnA-mediated dephosphorylation of NFAT in the cytosol, CnA also plays a role in the nucleus. There, CnA can sustain NFAT activity via a noncatalytic mechanism by associating with NFAT, occluding its nuclear export sequence and thereby maintaining its nuclear localization (Zhu and McKeon, 1999). Here, we find that nuclear CnA as well as elevated nuclear Ca^{2+} is required for IICR-induced ANF expression. As we also find that IICR-stimulated nuclear Ca^{2+} elevations increase nuclear NFAT, our data suggest that IICR engages CnA in the nucleus to enhance NFAT activation and hypertrophic gene transcription. Although our data show that $InsP_3$-stimuated increases in nuclear Ca^{2+} are required for induction of hypertrophy and NFAT accumulation in the nucleus, IICR may also elicit some of its actions in the perinuclear region of the cytosol. Interestingly, ET-1 stimulates GFP-CnA nuclear translocation in blocked cells (data not shown). Specificity in IICR signaling in this region as well as in the nucleus may be imparted through the reported physical interaction between CnA and $InsP_3Rs$ (Cameron et al., 1995).

Through its phosphorylation of HDACs, CaMKII has also been shown to be an important regulator of hypertrophic gene transcription (Zhang et al., 2002a; Zhang et al., 2002b). Indeed, IICR has been shown to activate nuclear-localized delta(b) isoform of CaMKII, inducing HDAC5 nuclear export and activation of a MEF2-luciferase reporter (Wu et al., 2006). As discussed earlier, whether IICR induces the expression of hypertrophy via this CaMK/HDAC pathway requires further investigation. We did not, however, detect sensitivity of ANF expression to CaMK inhibition (data not shown). CaMKII-dependent hypertrophy has been shown to be induced following isoproterenol treatment, although the requirement for IICR for hypertrophy on this background was not determined (Morisco et al., 2000). As hypertrophy is manifest through synergistic interactions between multiple signaling pathways (Heineke and Molkentin, 2006), it is likely that Ca^{2+} simultaneously coordinates numerous inputs during the induction of hypertrophy. Moreover, although we report that IICR is required for the induction of hypertrophy, IICR is unlikely to operate by itself in the induction of hypertrophic gene transcription. Concomitantly with induction of IICR, ET-1 receptor engagement would also lead to the activation, among others, of PKD, PKC, and MAPK signaling pathways (Dorn and Force, 2005; Sugden and Clerk, 2005). These signals would likely synergize with IICR to regulate gene transcription. The array of pathways involved in hypertrophy may also allow for redundancy; for example, under certain circumstances the requirement for IICR may be circumvented in the induction of hypertrophy.

To summarize, our data show that a signaling module involving ET-1-stimulated IICR and activation of NFAT plays a requisite and coordinating role in the induction of hypertrophic gene expression under conditions that increase cardiac work rate. The relevance of these findings to disease is immediately apparent. Specifically, the NFAT pathway is a well-defined and important regulator of pathological hypertrophy (Wilkins et al., 2004). Moreover, $InsP_3R$ expression (Go et al., 1995) and circulating ET-1 are increased during heart failure. Together, increases in the expression and/or activity of these signaling mediators could synergize to exacerbate the disease state. In addition, it is possible that IICR-associated arrhythmic events (Kockskamper et al., 2008) would also be increased, thereby compounding the severity of disease. These profound effects of ET-1 on the heart suggest that this pathway would be an attractive target for pharmacological intervention. Thus far, the responses of both animal and humans to ET receptor inhibitors have been inconsistent, possibly due to disease state or history (Ito et al., 1994). The antihypertrophic effect of deleting the *prepro-ET-1* gene in mice (Shohet et al., 2004) would suggest, however, that targeting the ET system in a cardiac-specific manner could prove beneficial.

EXPERIMENTAL PROCEDURES

Materials

Cell-permeant VIVIT peptide and porcine ET-1 were from Calbiochem. Chemicals were from Sigma or BDH, unless stated otherwise.

Preparation and Culture of Cardiac Myocytes

NRVMs were prepared and cultured as previously described with minor modifications (Iwaki et al., 1990) (see Supplemental Data). Following isolation and preplating to remove contaminating fibroblasts, myocytes were seeded at 0.2×10^6 cells/cm^2 in plating medium (4 parts DMEM with 4.5 g/l D-Glucose, 585 mg/l L-glutamine, 110 mg/l sodium pyruvate (Invitrogen) and 1 part M199, supplemented with 10% donor horse serum, 5% fetal calf serum, 1 mM sodium pyruvate, 1 mM MEM nonessential amino acids (Invitrogen), 1% antibiotic/antimycotic, and 3 μM cytosine b-D-arabinofuranoside (ara-C) on 1% gelatin-coated dishes or laminin (25 μg/ml; Invitrogen)-coated coverslips. Plating medium was replaced after 24 hr and left for a further 24 hr. Cells were then starved for 24 hr in maintenance medium (plating medium without serum and nonessential amino acids supplemented with 5.5 μg/ml transferrin, 5 ng/ml selenium). Myocyte cultures were >95% pure. Following starvation, cells were cultured in maintenance media for 24 hr, in the presence or absence of agonists/antagonists.

ARVMs were prepared as previously described (Lipp et al., 2000). For culture, myocytes were transferred into culture medium (M199 – HEPES modification, containing 0.2% BSA, 1.3 mM L-glutamine, 2.5 mM pyruvic acid, 5 mM creatine, 2 mM L-carnitine, 5 mM taurine, 5.5 μg/ml selenium, 3 μM ara-C and 1% antibiotic/antimycotic [Invitrogen]) and plated onto laminin-coated coverslips (25 μg/ml). After 2 hr, cells were exposed to the experimental manipulation and cultured for 20–24 hr in culture medium.

Generation of Nuclear Localized Calbindin

Expression vectors for nuclear-targeted (2× large T-antigen NLS) calbindin NH_2-terminally tagged with mRFP and for mRFP were prepared according

to standard procedures. cDNAs for rat calbindin and mRFP were provided by B. Schwaller (Fribourg, SZ) and R. Tsien (UCSD), respectively. Details are given in the Supplemental Data.

Real-Time Quantitative PCR

RNA was isolated from myocytes using the QIAGEN RNAeasy mini kit (with on column DNase treatment), according to the manufacturer's protocol. Total RNA (500 ng) was reverse transcribed with Superscript II reverse transcriptase (Invitrogen). Quantitative real-time PCR (qPCR) was performed using an ABI Prism 7700 Sequence Detection System using gene-specific primers that spanned exon boundaries and SYBR Green. Relative expression values were determined using the geNorm method (Vandesompele et al., 2002). Further details are in the Supplemental Data.

Immunofluorescence

Cells on coverslips were washed twice in PBS and then fixed for 15 min at 4°C in PBS (pH 7.4) containing 2% paraformaldehyde (w/v) and 0.05% glutaraldehyde (v/v). Cells were then washed three times with PBS and permeabilized in PBS containing 0.2% TRITON X-100 for 15 min. Autofluorescence was quenched with 1 mg/ml $NaBH_4$. Nonspecific protein binding sites were blocked by incubation for 1 hr in PBS/0.1% TRITON X-100/goat serum (5%, w/v) (blocking buffer). Primary antibodies—monoclonal anti-$InsP_3R2$ (Sugiyama et al., 1994) (1:250), polyclonal anti-RyR2 (1:100; gift of V. Sorrentino, University of Sienna), monoclonal anti-cardiac actinin (1:500; Sigma), and polyclonal anti-ANF (1:500; Peninsula Laboratories)—were diluted in blocking buffer and incubated with the cells for a further 1 hr. Excess antibody was removed by washing for 1 hr in PBS/0.1% TRITON X-100 (wash buffer). Bound antibodies were detected using Alexa Fluor-conjugated secondary antibodies (Invitrogen), which were diluted at 1:500 in wash buffer containing 0.2% goat serum and incubated with the cells for 1 hr. Excess secondary antibodies were removed by washing for 1 hr in wash buffer. Coverslips were mounted on slides using Vectashield ± DAPI. Cells were imaged using a Zeiss LSM 510META configured on an inverted microscope equipped with 40×, 1.3 n.a or 60×, 1.4 n.a oil immersion objectives, or on an Olympus Fluoview 1000 equipped with 40×, Plan apochromat 1.35 n.a. oil immersion objective.

Cell Size Measurements

Area measurements of confocal images of individual cells were determined using Volocity software (Improvision). For each condition, ≥100 cells on four or more coverslips (five fields of view per coverslip) from two or more preparations of cells were used.

Adenoviral Infection

Adenoviral vectors for GFP/cherry and GFP/cherry-tagged type 1 $InsP_3$ 5′-phosphatase were prepared with standard procedures using the flp/frt recombinase system (Microbix Biosystems Inc; see Supplemental Data for details of construct generation). Adenovirus for GFP-NFAT-C1 and NFAT-Luc were kind gifts of M. Schneider (University of Maryland) and J. Molkentin (University of Cincinnati), respectively, and have been described elsewhere (Liu et al., 2001; Wilkins et al., 2004). Viruses were purified using the Vivapure AdenoPack 100 viral purification kit (Sartorius). Viral titer was determined by OD or end-point dilution and used at a concentration that transduced greater than 95% of cells. For infection, virus was added in a minimal volume of media overlying the cells and incubated for 3 hr in the case of neonatal myocytes and overnight for adult myocytes. Virus-containing media was then removed and either replaced with media or media-containing agonist.

Transfection

Myocytes cultured in laminin-coated 16-well glass chamber slides were transfected in serum-free media. For transfection, 0.8 μg DNA, 2 μl Nupherin (BIOMOL), and 0.4 μl Lipofectamine LTX (Invitrogen) was used per well.

Ca^{2+} Imaging

Myocytes on glass coverslips were washed with imaging buffer (10 mM HEPES [pH 7.35], 135 mM NaCl, 5.4 mM KCl, 2 mM $MgCl_2$, 10 mM glucose, 1.5 mM $CaCl_2$) and then loaded with 2 μM fura-2 AM diluted in imaging buffer. Following 30 min incubation at 37°C, cells were washed and incubated for a further 25 min at 37°C to de-esterify the dye. The coverslips were then mounted in an imaging chamber and transferred to the temperature-controlled (37°C) stage of a Nikon TE200 inverted microscope. Cells were imaged through a 40×, 1.3 n.a. S Fluor oil immersion phase objective with alternate excitation at 340 and 380 nm. Light was filtered through a 400 nm long-pass dichroic and a 460 nm long-pass emission filter. Images were captured using a Hamamatsu Orca ER cooled CCD camera.

Confocal imaging of fluo-4-loaded myocytes was performed using an Olympus FluoView 1000 attached to an Olympus IX81. The cells were illuminated with the 488 nm line of an Argon/Krypton laser and imaged through a 40×, 1.3 n.a. UPlanFl oil immersion objective at 15.4 frames/s. For dye loading, cells were incubated with 2 μM fluo-4-AM at 37°C for 30 min followed by de-esterification at 37°C for a further 30 min. Cells were imaged in imaging buffer as described above for fura-2 imaging, but containing 1 mM $CaCl_2$ for ARVMs. Images were analyzed off-line using ImageJ software (http://rsb.info.nih.gov/ij/).

Assays of NFAT Activation

GFP-NFATC1 nuclear accumulation was quantitated 4 hr poststimulation with ET-1. Cells were fixed and immunostained with α-actinin. Myocytes with GFP-NFAT predominantly in the nucleus were classed as NFAT positive. NFAT-driven luciferase activity was determined 24 hr poststimulation using the Promega Luciferase Assay System.

ET-1 Enzyme Immunometric Assay

ET-1 was quantitated using an enzyme immunometric assay (EIA) kit (Assay Designs). The culture medium (900 μl) was removed from myocytes cultured in 6-well dishes (following 24 hr of treatment) and stored at −20°C. To achieve detectable ET-1 levels, samples from multiple preparations were pooled and then concentrated using Sep-Pak tC18 reversed-phase chromatography cartridges (Waters). Samples were eluted in 250 μl 50% MeOH/5% formic acid. Eluates were dried in a SpeedVac and resuspended in 220 μl of EIA assay buffer by incubation in a sonnicator water bath. The EIA was carried out as per the manufacturer's protocol.

Statistical Analysis

Data are presented as mean ± SEM. Data were analyzed using a one-tailed Student's t test or using a one-way ANOVA and Tukey post hoc test and were accepted as significant when $p < 0.05$.

SUPPLEMENTAL DATA

The Supplemental Data include Supplemental Experimental Procedures and three figures and can be found with this article online at http://www.cell.com/molecular-cell/supplemental/S1097-2765(09)00101-4.

ACKNOWLEDGMENTS

We are grateful to Stuart Conway (University of Oxford) for $InsP_3$-ester; M. Schneider, J. Molkentin, R. Tsien, C. Erneux, and B. Schwaller for cDNAs and viruses; and V. Sorrentino for anti-RyR2 Ab. The work was supported by The BHF (PG/07/040), The Babraham Institute, the MRC (studentship to D.R.H.), The Royal Society (University Research Fellowship to H.L.R.), and the BBSRC.

Received: November 23, 2007
Revised: October 24, 2008
Accepted: February 10, 2009
Published: February 26, 2009

REFERENCES

Allender, S., Peto, V., Scarborough, P., Boxer, A., and Raynor, M. (2006). Coronary Heart Disease Statistics (London: BHF).

Aramburu, J., Yaffe, M.B., Lopez-Rodriguez, C., Cantley, L.C., Hogan, P.G., and Rao, A. (1999). Affinity-driven peptide selection of an NFAT inhibitor more selective than cyclosporin A. Science *285*, 2129–2133.

Aronow, B.J., Toyokawa, T., Canning, A., Haghighi, K., Delling, U., Kranias, E., Molkentin, J.D., and Dorn, G.W., II. (2001). Divergent transcriptional responses to independent genetic causes of cardiac hypertrophy. Physiol. Genomics *6*, 19–28.

Berridge, M.J., Bootman, M.D., and Roderick, H.L. (2003). Calcium signalling: dynamics, homeostasis and remodelling. Nat. Rev. Mol. Cell Biol. *4*, 517–529.

Bers, D.M. (2002). Cardiac excitation-contraction coupling. Nature *415*, 198–205.

Brenner, J.S., and Dolmetsch, R.E. (2007). TrpC3 regulates hypertrophy-associated gene expression without affecting myocyte beating or cell size. PLoS ONE *2*, e802. 10.1371/journal.pone.0000802.

Cameron, A.M., Steiner, J.P., Roskams, A.J., Ali, S.M., Ronnett, G.V., and Snyder, S.H. (1995). Calcineurin associated with the inositol 1,4,5-trisphosphate receptor-FKBP12 complex modulates Ca^{2+} flux. Cell *83*, 463–472.

Cardenas, C., Liberona, J.L., Molgo, J., Colasante, C., Mignery, G.A., and Jaimovich, E. (2005). Nuclear inositol 1,4,5-trisphosphate receptors regulate local Ca^{2+} transients and modulate cAMP response element binding protein phosphorylation. J. Cell Sci. *118*, 3131–3140.

Colella, M., Grisan, F., Robert, V., Turner, J.D., Thomas, A.P., and Pozzan, T. (2008). Ca2+ oscillation frequency decoding in cardiac cell hypertrophy: role of calcineurin/NFAT as Ca2+ signal integrators. Proc. Natl. Acad. Sci. USA *105*, 2859–2864.

Dorn, G.W., II, and Force, T. (2005). Protein kinase cascades in the regulation of cardiac hypertrophy. J. Clin. Invest. *115*, 527–537.

Ergul, A., Walker, C.A., Goldberg, A., Baicu, S.C., Hendrick, J.W., King, M.K., and Spinale, F.G. (2000). ET-1 in the myocardial interstitium: relation to myocyte ECE activity and expression. Am. J. Physiol. Heart Circ. Physiol. *278*, H2050–H2056.

Escobar, A.L., Ribeiro-Costa, R., Villalba-Galea, C., Zoghbi, M.E., Perez, C.G., and Mejia-Alvarez, R. (2004). Developmental changes of intracellular Ca^{2+} transients in beating rat hearts. Am. J. Physiol. Heart Circ. Physiol. *286*, H971–H978.

Feske, S., Draeger, R., Peter, H.H., Eichmann, K., and Rao, A. (2000). The duration of nuclear residence of NFAT determines the pattern of cytokine expression in human SCID T cells. J. Immunol. *165*, 297–305.

Frey, N., McKinsey, T.A., and Olson, E.N. (2000). Decoding calcium signals involved in cardiac growth and function. Nat. Med. *6*, 1221–1227.

Go, L.O., Moschella, M.C., Watras, J., Handa, K.K., Fyfe, B.S., and Marks, A.R. (1995). Differential regulation of two types of intracellular calcium release channels during end-stage heart failure. J. Clin. Invest. *95*, 888–894.

Hallhuber, M., Burkard, N., Wu, R., Buch, M.H., Engelhardt, S., Hein, L., Neyses, L., Schuh, K., and Ritter, O. (2006). Inhibition of nuclear import of calcineurin prevents myocardial hypertrophy. Circ. Res. *99*, 626–635.

Hardingham, G.E., Chawla, S., Johnson, C.M., and Bading, H. (1997). Distinct functions of nuclear and cytoplasmic calcium in the control of gene expression. Nature *385*, 260–265.

Heidrich, F.M., Zhang, K., Estrada, M., Huang, Y., Giordano, F.J., and Ehrlich, B.E. (2008). Chromogranin B regulates calcium signaling, nuclear factor kappaB activity, and brain natriuretic peptide production in cardiomyocytes. Circ. Res. *102*, 1230–1238.

Heineke, J., and Molkentin, J.D. (2006). Regulation of cardiac hypertrophy by intracellular signalling pathways. Nat. Rev. Mol. Cell Biol. *7*, 589–600.

Hiebsch, R.R., Raub, T.J., and Wattenberg, B.W. (1991). Primaquine blocks transport by inhibiting the formation of functional transport vesicles. Studies in a cell-free assay of protein transport through the Golgi apparatus. J. Biol. Chem. *266*, 20323–20328.

Ito, H., Hiroe, M., Hirata, Y., Fujisaki, H., Adachi, S., Akimoto, H., Ohta, Y., and Marumo, F. (1994). Endothelin ETA receptor antagonist blocks cardiac hypertrophy provoked by hemodynamic overload. Circulation *89*, 2198–2203.

Iwaki, K., Sukhatme, V.P., Shubeita, H.E., and Chien, K.R. (1990). Alpha- and beta-adrenergic stimulation induces distinct patterns of immediate early gene expression in neonatal rat myocardial cells. fos/jun expression is associated with sarcomere assembly; Egr-1 induction is primarily an alpha 1-mediated response. J. Biol. Chem. *265*, 13809–13817.

Kockskamper, J., Zima, A.V., Roderick, H.L., Pieske, B., Blatter, L.A., and Bootman, M.D. (2008). Emerging roles of inositol 1,4,5-trisphosphate signaling in cardiac myocytes. J. Mol. Cell. Cardiol. *45*, 128–147.

Kuwahara, K., Wang, Y., McAnally, J., Richardson, J.A., Bassel-Duby, R., Hill, J.A., and Olson, E.N. (2006). TRPC6 fulfills a calcineurin signaling circuit during pathologic cardiac remodeling. J. Clin. Invest. *116*, 3114–3126.

Lipp, P., Laine, M., Tovey, S.C., Burrell, K.M., Berridge, M.J., Li, W., and Bootman, M.D. (2000). Functional InsP3 receptors that may modulate excitation-contraction coupling in the heart. Curr. Biol. *10*, 939–942.

Liu, Y., Cseresnyes, Z., Randall, W.R., and Schneider, M.F. (2001). Activity-dependent nuclear translocation and intranuclear distribution of NFATc in adult skeletal muscle fibers. J. Cell Biol. *155*, 27–39.

Lorell, B.H., and Carabello, B.A. (2000). Left ventricular hypertrophy: pathogenesis, detection, and prognosis. Circulation *102*, 470–479.

Mackenzie, L., Bootman, M.D., Laine, M., Berridge, M.J., Thuring, J., Holmes, A., Li, W.H., and Lipp, P. (2002). The role of inositol 1,4,5-trisphosphate receptors in $Ca^{(2+)}$ signalling and the generation of arrhythmias in rat atrial myocytes. J. Physiol. *541*, 395–409.

Molkentin, J.D. (2006). Dichotomy of Ca^{2+} in the heart: contraction versus intracellular signaling. J. Clin. Invest. *116*, 623–626.

Molkentin, J.D., Lu, J.R., Antos, C.L., Markham, B., Richardson, J., Robbins, J., Grant, S.R., and Olson, E.N. (1998). A calcineurin-dependent transcriptional pathway for cardiac hypertrophy. Cell *93*, 215–228.

Morisco, C., Zebrowski, D., Condorelli, G., Tsichlis, P., Vatner, S.F., and Sadoshima, J. (2000). The Akt-glycogen synthase kinase 3beta pathway regulates transcription of atrial natriuretic factor induced by beta-adrenergic receptor stimulation in cardiac myocytes. J. Biol. Chem. *275*, 14466–14475.

Motte, S., van Beneden, R., Mottet, J., Rondelet, B., Mathieu, M., Havaux, X., Lause, P., Clercx, C., Ketelslegers, J.M., Naeije, R., and McEntee, K. (2003). Early activation of cardiac and renal endothelin systems in experimental heart failure. Am. J. Physiol. Heart Circ. Physiol. *285*, H2482–H2491.

Nakayama, H., Wilkin, B.J., Bodi, I., and Molkentin, J.D. (2006). Calcineurin-dependent cardiomyopathy is activated by TRPC in the adult mouse heart. FASEB J. *20*, 1660–1670.

Obata, K., Nagata, K., Iwase, M., Odashima, M., Nagasaka, T., Izawa, H., Murohara, T., Yamada, Y., and Yokota, M. (2005). Overexpression of calmodulin induces cardiac hypertrophy by a calcineurin-dependent pathway. Biochem. Biophys. Res. Commun. *338*, 1299–1305.

Perez, P.J., Ramos-Franco, J., Fill, M., and Mignery, G.A. (1997). Identification and functional reconstitution of the type 2 inositol 1,4,5-trisphosphate receptor from ventricular cardiac myocytes. J. Biol. Chem. *272*, 23961–23969.

Russell, F.D., and Molenaar, P. (2000). The human heart endothelin system: ET-1 synthesis, storage, release and effect. Trends Pharmacol. Sci. *21*, 353–359.

Shohet, R.V., Kisanuki, Y.Y., Zhao, X.S., Siddiquee, Z., Franco, F., and Yanagisawa, M. (2004). Mice with cardiomyocyte-specific disruption of the endothelin-1 gene are resistant to hyperthyroid cardiac hypertrophy. Proc. Natl. Acad. Sci. USA *101*, 2088–2093.

Shubeita, H.E., McDonough, P.M., Harris, A.N., Knowlton, K.U., Glembotski, C.C., Brown, J.H., and Chien, K.R. (1990). Endothelin induction of inositol phospholipid hydrolysis, sarcomere assembly, and cardiac gene expression in ventricular myocytes. A paracrine mechanism for myocardial cell hypertrophy. J. Biol. Chem. *265*, 20555–20562.

Song, K., Backs, J., McAnally, J., Qi, X., Gerard, R.D., Richardson, J.A., Hill, J.A., Bassel-Duby, R., and Olson, E.N. (2006). The transcriptional coactivator CAMTA2 stimulates cardiac growth by opposing class II histone deacetylases. Cell *125*, 453–466.

Sugden, P.H., and Clerk, A. (2005). Endothelin signalling in the cardiac myocyte and its pathophysiological relevance. Curr. Vasc. Pharmacol. *3*, 343–351.

Sugiyama, T., Furuya, A., Monkawa, T., Yamamoto-Hino, M., Satoh, S., Ohmori, K., Miyawaki, A., Hanai, N., Mikoshiba, K., and Hasegawa, M. (1994). Monoclonal antibodies distinctively recognizing the subtypes of inositol 1,4,5-trisphosphate receptor: application to the studies on inflammatory cells. FEBS Lett. *354*, 149–154.

Tomida, T., Hirose, K., Takizawa, A., Shibasaki, F., and Iino, M. (2003). NFAT functions as a working memory of Ca^{2+} signals in decoding Ca^{2+} oscillation. EMBO J. *22*, 3825–3832.

Vandesompele, J., De Preter, K., Pattyn, F., Poppe, B., Van Roy, N., De Paepe, A., and Speleman, F. (2002). Accurate normalization of real-time quantitative RT-PCR data by geometric averaging of multiple internal control genes. Genome Biol. *3*, RESEARCH0034.

Wettschureck, N., Rutten, H., Zywietz, A., Gehring, D., Wilkie, T.M., Chen, J., Chien, K.R., and Offermanns, S. (2001). Absence of pressure overload induced myocardial hypertrophy after conditional inactivation of Galphaq/Galpha11 in cardiomyocytes. Nat. Med. *7*, 1236–1240.

Wilkins, B.J., Dai, Y.S., Bueno, O.F., Parsons, S.A., Xu, J., Plank, D.M., Jones, F., Kimball, T.R., and Molkentin, J.D. (2004). Calcineurin/NFAT coupling participates in pathological, but not physiological, cardiac hypertrophy. Circ. Res. *94*, 110–118.

Wu, X., Zhang, T., Bossuyt, J., Li, X., McKinsey, T.A., Dedman, J.R., Olson, E.N., Chen, J., Brown, J.H., and Bers, D.M. (2006). Local InsP3-dependent perinuclear Ca^{2+} signaling in cardiac myocyte excitation-transcription coupling. J. Clin. Invest. *116*, 675–682.

Zhang, C.L., McKinsey, T.A., Chang, S., Antos, C.L., Hill, J.A., and Olson, E.N. (2002a). Class II histone deacetylases act as signal-responsive repressors of cardiac hypertrophy. Cell *110*, 479–488.

Zhang, T., Johnson, E.N., Gu, Y., Morissette, M.R., Sah, V.P., Gigena, M.S., Belke, D.D., Dillmann, W.H., Rogers, T.B., Schulman, H., et al. (2002b). The cardiac-specific nuclear delta(B) isoform of Ca^{2+}/calmodulin-dependent protein kinase II induces hypertrophy and dilated cardiomyopathy associated with increased protein phosphatase 2A activity. J. Biol. Chem. *277*, 1261–1267.

Zhu, J., and McKeon, F. (1999). NF-AT activation requires suppression of Crm1-dependent export by calcineurin. Nature *398*, 256–260.

Zima, A.V., Bare, D.J., Mignery, G.A., and Blatter, L.A. (2007). IP3-dependent nuclear Ca signaling in the heart. J. Physiol. *584*, 601–611.

Zima, A.V., and Blatter, L.A. (2004). Inositol-1,4,5-trisphosphate-dependent $Ca^{(2+)}$ signalling in cat atrial excitation-contraction coupling and arrhythmias. J. Physiol. *555*, 607–615.

Zolk, O., Quattek, J., Seeland, U., El-Armouche, A., Eschenhagen, T., and Bohm, M. (2002). Activation of the cardiac endothelin system in left ventricular hypertrophy before onset of heart failure in TG(mREN2)27 rats. Cardiovasc. Res. *53*, 363–371.